on Si(001) should be good candidates because they have a dimer row structure.

At room temperature, the small structures we have made are stable for as long as we have observed them (several hours). We can roughly estimate their thermal stability from available values of the activation energies for desorption of dimers from S_A (*17, 18*) and S_B steps (*17–19*). Bridges that have only S_A edges (Fig. 6) decompose most easily by removal of a dimer from an S_A edge. The theoretical value of the energy required for this process is ~2.1 eV (*17*). If we use an Arrhenius relation with an attempt frequency of 10^{13} s^{-1}, the predicted decay rate at room temperature is one defect created in $\sim 10^{10}$ years. However, the time to create one defect becomes only ~1 min at 325°C, a moderate temperature by the standard of present semiconductor processing. For the island structure (Fig. 5), the easiest decomposition mechanism is the removal of dimers from the ends of rows. Experimental (*19*) and theoretical (*18*) investigations yield an estimate of 1.4 to 1.7 eV for the energy to remove a dimer from an S_B edge. If we use 1.5 eV as a mean value, the average time to create one defect is ~100 years at room temperature and ~10 ms at 325°C. These estimates indicate that the issue of structural integrity will play an important role in any potential technological use of atomic-scale silicon structures. Possible solutions to the stability problem include inducing chemical stabilization, burying the structures, or processing at lower temperatures than those used today.

REFERENCES AND NOTES

1. J. A. Stroscio and D. M. Eigler, *Science* **254**, 1319 (1991).
2. S. Hosoki, S. Hosaka, T. Hasegawa, *Appl. Surf. Sci.* **60/61**, 643 (1992).
3. M. Aono, A. Kobayashi, F. Grey, H. Uchida, D. Huang, *Jpn. J. Appl. Phys.* **32**, 1470 (1993).
4. M. F. Crommie, C. P. Lutz, D. M. Eigler, *Science* **262**, 218 (1993).
5. D. M. Eigler, C. P. Lutz, W. E. Rudge, *Nature* **352**, 600 (1991).
6. R. S. Becker, J. A. Golovchenko, B. S. Swartzentruber, *ibid.* **325**, 419 (1987).
7. H. J. Mamin, S. Chiang, H. Birk, P. H. Guethner, D. Rugar, *J. Vac. Sci. Technol. B* **9**, 1398 (1991).
8. R. M. Silver, E. E. Ehrichs, A. L. de Lozanne, *Appl. Phys. Lett.* **51**, 247 (1987).
9. W. Li, J. A. Virtanen, R. M. Penner, *ibid.* **60**, 1181 (1992).
10. M. A. McCord and R. F. W. Pease, *J. Vac. Sci. Technol. B* **5**, 430 (1987).
11. J. A. Dagata *et al.*, *Appl. Phys. Lett.* **56**, 2001 (1990).
12. I.-W. Lyo and Ph. Avouris, *Science* **253**, 173 (1991).
13. A. Kobayashi, F. Grey, R. S. Williams, M. Aono, *ibid.* **259**, 1724 (1993).
14. Y. Hasegawa and Ph. Avouris, *ibid.* **258**, 1763 (1992).
15. B. S. Swartzentruber, Y.-W. Mo, M. B. Webb, M. G. Lagally, *J. Vac. Sci. Technol. A* **7**, 2901 (1989).
16. B. S. Swartzentruber, Y.-W. Mo, R. Kariotis, M. G. Lagally, M. B. Webb, *Phys. Rev. Lett.* **65**, 1913 (1990).
17. Z. Y. Zhang, H. Chen, B. C. Bolding, M. G. Lagally, *ibid.* **71**, 3677 (1993).
18. Z. Y. Zhang, unpublished results.
19. N. Kitamura, B. S. Swartzentruber, M. G. Lagally, M. B. Webb, *Phys. Rev. B* **48**, 5704 (1993).

20. This research was supported by NSF grant DMR 93-04912 and by the Air Force Office of Scientific Research. We thank J. Vasek and F. Wu for help with the experiments and P. Avouris, N. Kitamura, and Z. Y. Zhang for useful discussions.

25 March 1994; accepted 6 June 1994

Fluctuations and Supercoiling of DNA

John F. Marko* and Eric D. Siggia

Frequently, DNA in vivo is organized into loops that are partially underwound and consequently form interwound helical supercoils. Methods from polymer statistical mechanics are used to show how the competition between entropy (thermal fluctuations) and elastic energy determines supercoil radius and pitch, in good agreement with recent experiments and simulations. Supercoil reorganization by means of slithering (reptation) of the DNA along the supercoil is argued to be a slow process. Extension of supercoiled DNA by an applied force shows a number of unexpected features, including coexistence of interwound and helical states.

Closed loops of double-stranded DNA are ubiquitous in organisms ranging from certain viruses and prokaryotes, in which the entire genome (or accompanying plasmids) is a single loop, to eukaryotes, in which chromosomes are organized by DNA-binding proteins into 50- to 100-kb loops (*1–3*). These loops change conformation subject to topological constraints, such as the double-helix linking number Lk (*4, 5*), which is conserved as long as the strands remain unbroken. The conformational biases induced by the Lk constraint are manifest in the writhing or supercoiling of the molecule, analogous to the familiar buckling of a twisted tube or wire. Supercoiling is believed to play a biological role in that elaborate cellular machinery has evolved to manipulate Lk either by direct enzymatic action or more indirectly by binding to particular proteins (*1*).

Conventionally, linking number perturbations of a loop of length L are reported with a fractional linking number $\sigma = Lk/Lk_0 - 1$, where $Lk_0 = L/h$ is the number of helix repeats along an open chain of length L; for B-form DNA, h = 3.4 nm (*1*). Except in thermophilic bacteria, σ is negative and approximately equal to −0.05. Further unwinding of the double helix to $\sigma < -0.10$ unbinds the strands.

The many studies of elastic equilibria (6) of loops with $\sigma \neq 0$ are of limited relevance to the situations encountered biologically because DNA loops are typically much longer than the thermal persistence lengths, which are on the order of 50 nm. Arduous Monte Carlo computer simulations (*7*) have correctly accounted for thermal fluctuations and have achieved impressive agreement with experiment (*8*), except in cases where cation-induced condensation may play a role (*9*). In this report, we reproduce the results of two previous reports (*7, 8*) semiquantitatively by simple statistical-mechanical calculations that provide useful insight into how entropy and elastic energy compete to determine the observed supercoil structure. In addition, several experimentally testable predictions are made.

The energy (enthalpy) of deformation of the double helix (*5*) depends on its local curvature $\kappa(s)$ and local excess twist $\Omega(s)$, both of which have units of inverse length and depend on s, the arc length along the axis of the molecule. The energy per unit length in units of k_BT (where k_B is Boltzmann's constant and T is temperature) is $\epsilon = \frac{1}{2}(A\kappa^2 + C\Omega^2)$ (*10*), where $A \approx 50$ nm and $C \approx 75$ nm are the persistence lengths for bends and twists, respectively (*11*). The total molecular twist (*2, 3*) is

$$Tw = \int_0^L ds[\omega_0 + \Omega(s)]/2\pi \qquad (1)$$

where $\omega_0 = 2\pi/h = 1.85$ nm^{-1} is the local twist of an undistorted molecule. The values of Tw and Lk are related by $Lk = Tw + Wr$, where Wr is the "writhe" of the molecule (*4, 5*), a quantity independent of $\Omega(s)$.

The probability distribution of conformations is given by the Boltzmann distribution $\exp[-\int ds\, \epsilon(s)]$. The Ω dependence can be explicitly averaged out and reexpressed with the constraint $Tw = Lk - Wr$. However, the remaining average over backbone conformation is complex and has only been implemented numerically (*7, 12*).

For small $|\sigma|$, perturbation theory around a free untwisted chain is reasonable, provided that the number of added links per twist persistence length, $X = C\omega_0|\sigma| \approx 130|\sigma|$, is less than about unity. The excess free energy

Laboratory for Atomic and Solid State Physics, Clark Hall, Cornell University, Ithaca, NY 14853–2501, USA.

*Present address: Center for Theoretical Studies in Physics and Biology, The Rockefeller University, 1230 York Avenue, New York, NY 10021–6399, USA.

per length f attributable to supercoiling thus behaves as $f/k_BT = \alpha_f X^2/C$, and the writhe per added linking is $Wr/\Delta Lk = \alpha_W$ plus a term on the order of X^2 (*13*). It is natural to use X rather than $|\sigma|$ because we expect strong conformational changes for $X \geq 1$.

For $X > 1$, a simple calculation is feasible if one adopts as a starting point a local superhelical reference state, as suggested by both mechanical experiments with twisted wires and Monte Carlo simulations. The all-important entropic contributions to f are calculated from Gaussian fluctuations around a regular solenoidal or plectonemic superhelix with an assumed pitch P and radius R. The optimal structure is then derived by minimizing f with respect to superhelix type, P, and R (Fig. 1).

The bend and twist energetic contributions to f are readily estimated from the curvature $\kappa = R/(P^2 + R^2)$, the constraint $Tw = Lk - Wr$, and the average supercoil writhe

$$Wr = \begin{cases} \mp n \sin\gamma & \text{plectoneme} \\ \pm n(1 - \sin\gamma) & \text{solenoid} \end{cases} \quad (2)$$

where γ is the superhelix opening angle and n is the number of superhelical turns along the supercoil [$\sin\gamma = P/\sqrt{R^2 + P^2}$; $n = L/(2\pi\sqrt{R^2 + P^2})$]. The upper and lower signs refer to right- and left-handed superhelices, respectively.

The energy of the plectoneme can be reduced to zero if we put all of the excess linking into the writhe (thus making the twist energy vanish), which for given n is maximum for $\sin\gamma = 1$ or $R/P \to 0$. This makes curvature κ and the bending energy zero. On the other hand, the solenoid can have its twist energy reduced to zero at minimal curvature energy cost by collapsing the coils into the plane ($\sin\gamma = 0$). However, a bending contribution to the energy, $2\pi^2n^2A/L$, remains that is still positive and extensive, illustrating why twisted wire loops form plectonemes rather than solenoids. We show below that, although it is energetically costly, the solenoid state occurs when a twisted wire is subject to tension.

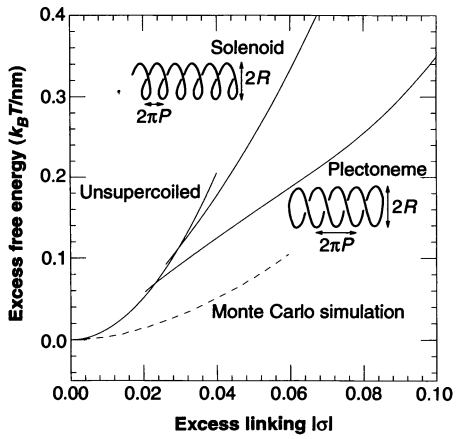

Fig. 1. Excess free energies per unit length versus excess linking number σ for regular solenoid and plectoneme supercoils with radius R and pitch P as drawn. The plectoneme state ceases to exist as a local minimum of Eq. 4 below $|\sigma| = 0.02$ and crosses the energy of the unsupercoiled state for $|\sigma| = 0.023$. The Monte Carlo energy (*7*) is systematically lower because we neglect the random coil entropy.

Any physical wire cannot collapse to less than its hard core radius, which for DNA in solution at biological ionic strengths (~140 mM Na^+) is $r_0 \approx 2$ nm (*14*). Simulations by Vologodskii *et al.* (*7*) and experiments (*3*, *8*) agree that plectoneme radii are much larger than r_0 until X exceeds 10. The central point of this report is that plectonemes swell as a result of thermal fluctuations; reducing R requires the suppression of fluctuations, which causes a loss of entropy.

This entropy loss may be estimated with the scaling ideas originally developed for the study of fluctuating membranes (*15*). We present a rough estimate for the plectoneme case that agrees with a systematic Gaussian calculation (*16*). When $R \ll P$, steric hindrance limits the distance that any portion of the molecule can fluctuate away from the average regular superhelix to R. This constraint on the fluctuations reduces the correlation length ξ along the double helix for the bending fluctuations. To find the relation between ξ and R, we must consider the energy of a fluctuation $\mathbf{a}(s)$ away from an average superhelical configuration.

If we use the normal modes $\mathbf{a}_k = \int ds\, e^{iks}\mathbf{a}(s)$, the bending energy is a sum over contributions for each wave number k with a leading term that scales as $k_BTAk^4|\mathbf{a}_k|^2$. Equipartition indicates that in thermal equilibrium, $\langle|\mathbf{a}_k|^2\rangle \approx 1/(Ak^4)$ for $k > \xi^{-1}$. For $k < \xi^{-1}$, the fluctuations are suppressed, and we may take $\langle|\mathbf{a}_k|^2\rangle = 0$ in this range. Therefore, the average of the square of the fluctuation at any point s along the supercoil is

$$\langle \mathbf{a}^2(s)\rangle \approx \int_{\xi^{-1}}^{\infty} \frac{dk}{Ak^4} \approx \frac{\xi^3}{A} \quad (3)$$

Our observation that the fluctuation amplitude is R gives the relation $\xi^3 \approx AR^2$. Finally, the confinement free energy per unit length scales as $k_BT/\xi = k_BTA^{-1/3}R^{-2/3}$. A similar argument applied to the solenoid case (for $\pi P \ll R$) gives a confinement free energy per unit length of $k_BT\,A^{-1/3}(\pi P)^{-2/3}$.

The free energy per unit length for a supercoil with $X > 1$ therefore has the form, to within order-unity constants

$$f/k_BT = A\kappa^2/2 + C\Omega^2/2 + A^{-1/3}[R^{-2/3} + (\pi P)^{-2/3}] + [(R/r_0)^{-12} + (\pi P/r_0)^{-12}]/r_0 \quad (4)$$

The first two terms are the static bend and twist energies noted above, the third term is a sum of the entropic penalty incurred as either or both of R and P are reduced to zero, and the final term models the short-ranged hard core interaction. The recent proposal (*9*) of salt-induced supercoil collapse could be modeled by including an attractive potential tail with the hard core. Because $Tw = Lk - Wr$, the excess twist is

$$\Omega = \omega_0\sigma \pm P/(R^2 + P^2) \quad (5)$$

for the plectoneme and

$$\Omega = \omega_0\sigma \pm P/(R^2 + P^2) \mp 1/\sqrt{R^2 + P^2} \quad (6)$$

for the solenoid. Given X, minimization of this free energy with respect to R and P yields the equilibrium structure.

For small X, the equilibrium state has $R = P = \infty$, indicating an unsupercoiled conformation. As X is increased to $X_0 = 3.0$ (with numerical constants as in Eq. 4), the equilibrium state jumps to that of a plectonemic superhelix with finite R and P, as observed experimentally and in simulations (*17*) (Fig. 1). Because a polymer is one dimensional, we expect that the sharp transition with increasing X between the unsupercoiled state and the plectoneme is smoothed out by thermal fluctuations. Our results lie systematically above the Monte Carlo results (*7*) because Eq. 4 does not include random coil entropy of order $-k_BT/A$. The absolute scale and the variation of the plectoneme parameters with σ observed experimentally (*8*) are described well by our model (Fig. 2), indicating that the free energy cost of

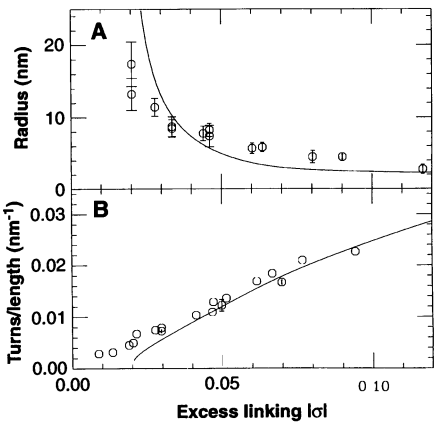

Fig. 2. Plectonemic supercoil (**A**) radius R and (**B**) turns per unit length $1/[2\pi(R^2 + P^2)^{1/2}]$ versus σ from Eq. 4 (solid lines) and experiments on 3.5-kb plasmids. The experimental R values [figure 12 of (*8*)] were derived from a direct measurement of the number of turns [figure 6 of (*8*)], the length of plectoneme axis, the number of ends, and L. No attempt was made to adjust the unknown order-unity constants in Eq. 4 to improve the fit.

confinement determines supercoil size.

For $X \gg 1$, simple scaling laws for all quantities can be derived from Eq. 4. The plectoneme free energy grows as $f/k_BT \approx X/C$, which is much less at large X than that of the solenoid, $f/k_BT \approx X^2/C$. This difference explains why the plectonemic coil is the stable state for $X > 1$. The plectoneme radius and pitch scale as $R \approx C/X^{3/2}$ and $P \approx C/X$. This scaling behavior is cut off for small $X \approx 1$ by strong corrections from random coil fluctuations and at high X by the hard core interactions. The large-X cutoff thus occurs for $R \approx r_0$, or for $X \approx (C/r_0)^{2/3} \approx 10$, and causes the upturn in the plectoneme free energy (Fig. 1). Similar scaling laws have been experimentally determined [R and $P \approx 1/X$ (*3*)], and our model provides a framework for understanding their origin.

Plectonemic supercoils have a branched structure (*8*), and they can be considered to be "living" branched polymers (*18*). We can roughly estimate the distance between branches for $X > 1$ by noting that the free energy required to create a "Y" branch point is that needed to create a random-coil region of length ξ, which is $\sim k_BTX$, a behavior that has been observed in simulations (*7*). If the interbranch distance λ is much larger than P, the entropy per branch will scale as $k_B \log \lambda/P$, and thus, balancing energy cost with entropic gain, we expect $\lambda \approx (C/X)\exp(\gamma X)$, where γ is a constant of order unity. By taking $\gamma \approx 1$ and moderate $X \approx 5$, we have $\lambda \approx 2000$ nm, compatible with simulation results (*7*).

A plectonemic supercoil brings into proximity sites separated by many base pairs along a DNA loop, so it is natural to suppose that the slithering or conveyor belt–like motion of DNA through the supercoil increases the rate of protein-mediated intramolecular reactions or fluorescence transfer in vitro (*19*). Such is not the case. For an open coil in solvent of viscosity η, ignoring self-avoidance interactions (reasonable for DNA shorter than 250 kb), the reaction time is $\tau_0 = 25(L/A)^{3/2}\eta A^3/k_BT$ (*20*). For the slithering of DNA around an unbranched plectoneme, we compute the ratio of drag force to velocity, μ, on two parallel cylinders of radius r_0, spacing R, and length $L/2$ to be $\mu = 2\pi\eta L/\log(R/r_0)$. The reaction time is thus $\tau_P = L^2\mu/k_BT$, which greatly exceeds τ_0 for $L \gg A$. However, intramolecular reactions can also occur through bending of the branched plectoneme of effective length $\sim L/2$ and stiffness $\sim 2A$. For $|\sigma| \approx 0.05$, we estimate a consequent reaction time ranging from τ_0 for $L \leq 5$ kb to $\sim 0.5\tau_0$ for $L \geq 50$ kb; the slight decrease in reaction time relative to τ_0 results from plectoneme branching, which increases the polymer density (*16*).

Recently, force versus extension measurements were made on a single DNA molecule (*21*), and it is tempting to anticipate what will happen if the experiments are repeated with a nonzero σ imposed. Because the energetically preferred plectoneme phase is unable to traverse distance, whatever extension exists must be bridged by a helical random coil or solenoid. Extension thus brings the solenoidal and plectonemic states into "phase coexistence."

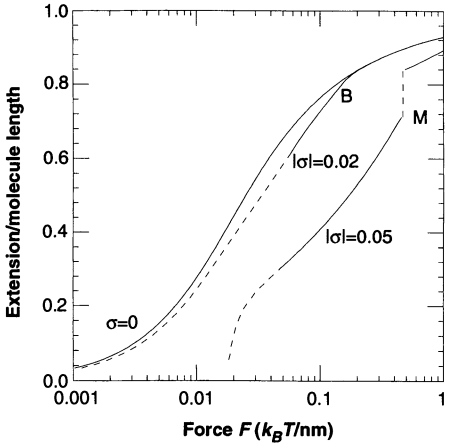

Fig. 3. Extension versus force for DNA with fixed linking number (note 1 k_BT/nm $\approx 4 \times 10^{-12}$ N). The $\sigma = 0$ calculation is exact, whereas the other curves are calculated in the large force limit, which, in the case of small $|\sigma|$, results in errors $\leq$5% for extensions $\geq$0.3. A plectonemic bubble appears with decreasing F at point B ($|\sigma| = 0.02$), and for larger $|\sigma|$, the concentration of links in the plectonemic phase causes the DNA to unbind or melt at point M as F increases.

The calculated extension versus force F (*16*) is shown in Fig. 3. Although the increase of F with $|\sigma|$ at fixed extension is intuitively plausible, the radius, pitch, and σ of each component phase in the mixed "plecto-noid" state, which we also calculate, are less easy to divine. For $|\sigma| = 0.02$ a large force eliminates all net writhe, the link is entirely twist, and the extension is identical to that of a $\sigma = 0$ random coil. As F decreases, some of the twist is expelled into a small plectonemic bubble with $|\sigma_P| \sim 0.08$, which grows to $\sim$8% of L for a fractional extension of 0.5, at which point the calculation becomes unreliable. We expect the plectoneme phase to vanish entirely as $F \rightarrow 0$ because a closed loop takes on chiral random coil conformations at this σ.

For larger $|\sigma|$, for example 0.05, when the $F = 0$ state is plectonemic, a finite force (equivalent to a free energy per length) must be exerted to have any extension at all. As F increases, there is again a tendency to concentrate σ in the plectoneme phase, but now $|\sigma_P|$ can exceed 0.12, which we take somewhat arbitrarily to be the point where DNA unbinds. These transitions could also occur whenever DNA is pinned at two locations and subject to twist as in the bacterial nucleoid; thus, extension of the force measurements of Smith *et al.* (*21*) to nonzero σ should prove interesting.

REFERENCES AND NOTES

1. A. P. Wolffe, *Chromatin* (Academic Press, New York, 1993).
2. A. D. Bates and A. Maxwell, *DNA Topology* (Oxford Univ. Press, Oxford, 1993), chap. 4 and references therein.
3. N. R. Cozzarelli, T. C. Boles, J. White, in *DNA Topology and Its Biological Effects*, N. R. Cozzarelli and J. C. Wang, Eds. (Cold Spring Harbor Laboratory, Cold Spring Harbor, NY, 1990), chap. 4.
4. J. H. White, *Am. J. Math.* **91**, 693 (1969).
5. F. B. Fuller, *Proc. Natl. Acad. Sci. U.S.A.* **68**, 815 (1971).
6. M. Le Bret, *Biopolymers* **18**, 1709 (1979); C. J. Benham, *ibid.* **22**, 2477 (1983); M. Le Bret, *ibid.* **23**, 1835 (1984); F. Tanaka and H. Takahashi, *J. Chem. Phys.* **83**, 6017 (1985).
7. A. V. Vologodskii, S. D. Levene, K. V. Klenin, M. Frank-Kamenetskii, N. R. Cozzarelli, *J. Mol. Biol.* **227**, 1224 (1992).
8. T. C. Boles, J. H. White, N. R. Cozzarelli, *ibid.* **213**, 931 (1990).
9. J. Bednar *et al.*, *ibid.* **235**, 825 (1994).
10. This model is suitable for B-form DNA because of its inherent bend and twist stiffness. The state $\kappa = \Omega = 0$ is the minimum energy conformation, a straight rod with regular helix repeat h.
11. Measurement of A by a variety of groups yields values close to 50 nm [P. J. Hagerman, *Annu. Rev. Biophys. Biophys. Chem.* **17**, 265 (1988)]. Values for C determined experimentally range from 40 to 100 nm [W. H. Taylor and P. J. Hagerman, *J. Mol. Biol.* **212**, 363 (1990); D. M. Crothers, J. Drak, J. D. Kahn, S. D. Levene, *Methods Enzymol.* **212**, 3 (1992)]. All calculations in this report use $A = 50$ nm and $C = 75$ nm, as in (*7*).
12. T. Schlick and W. Olson, *J. Mol. Biol.* **223**, 1089 (1992).
13. The numbers α_t and α_w depend on A and C; we estimate $\alpha_t \approx 0.31$ and $\alpha_w \approx 0.72$ using the numerical results of (*7*).
14. The hard core range r_0 is determined predominantly by electrostatic repulsion and thus varies with ionic strength [S. Y. Shaw and J. C. Wang, *Science* **260**, 533 (1993); V. V. Rybenkov, N. R. Cozzarelli, A. V. Vologodskii, *Proc. Natl. Acad. Sci. U.S.A.* **90**, 5307 (1993)]. All computations here use $r_0 = 1.75$ nm, as in (*7*).
15. Stacked fluctuating membranes have a power law interaction because their fluctuation entropy is reduced as they are pushed together [W. Helfrich, *Z. Naturforsch. Teil A* **33**, 305 (1978); S. Leibler, in *Statistical Mechanics of Membranes and Surfaces*, vol. 5 of *Jerusalem Winter School for Theoretical Physics*, D. Nelson, T. Piran, S. Weinberg, Eds. (World Scientific, Teaneck, NJ, 1989), pp. 81–82].
16. J. F. Marko and E. D. Siggia, unpublished results.
17. On p. 946 of (*8*), such a transition is reported for $|\sigma| = 0.019$; figure 14 of (*7*) shows that the entropy (essentially the number of conformations of the backbone) remains at its $\sigma = 0$ value for $|\sigma| \leq 0.02$.
18. M. Daoud and J. F. Joanny, *J. Phys. (Paris)* **42**, 1359 (1981).
19. C. N. Parker and S. E. Halford, *Cell* **66**, 781 (1991); H. A. Benjamin and N. R. Cozzarelli, *Proc. Robert A. Welch Found. Conf. Chem. Res.* **29**, 107 (1986).
20. M. Doi, *Chem. Phys.* **11**, 115 (1975); O. G. Berg, *Biopolymers* **23**, 1869 (1984). We have omitted the weak dependence of τ_0 on reaction site radius; this is incorporated into the prefactor.
21. S. B. Smith, L. Finzi, C. Bustamante, *Science* **258**, 1122 (1992).

22. Our research was supported by the NSF under grant DMR-9012974.

31 March 1994; accepted 3 June 1994